

Optical Nonlinearities in Crystalline Organic Multiple Quantum Wells

Juan F. Lam,⁽¹⁾ Stephen R. Forrest,⁽²⁾ and Gregory L. Tangonan⁽¹⁾

⁽¹⁾*Hughes Research Laboratories, Malibu, California 90265*

⁽²⁾*Center for Photonic Technology, Departments of Electrical Engineering and Materials Science, University of Southern California, Los Angeles, California 90089-0241*

(Received 2 November 1990)

A study of the linear and nonlinear optical behavior of recently realized crystalline organic semiconductor quantum wells is reported. Using the Davydov Hamiltonian, we find analytical solutions for the optical response function, and we predict the existence of intrinsic optical bistability and two-beam-coupling energy transfer in these materials.

PACS numbers: 72.80.Le, 78.20.-e

Current research in the optical properties of organic materials has been directed toward the elucidation of the dominant mechanism that gives rise to their nonlinear optical behavior.¹ In spite of the many experiments performed over the past decade,² little depth of understanding has been achieved. The complications arise from the competing effects between the delocalization of the photogenerated charge carriers,³ and formation of the excitations or quasiparticles.⁴ Recent nonlinear optical-absorption experiments⁵ performed on the quasi-1D semiconductor polydiacetylene appeared to confirm the concept⁶ that excitons are responsible for the nonlinear optical behavior of 1D organic materials.

In this work, we have extended the studies of semiconductor multiple quantum wells (MQWs) to the case of crystalline organic MQWs (CO-MQWs) (Ref. 7) and have found that the response of the quantum-confined charge-transfer (CT) excitons to external fields have novel nonlinear optical properties. CT excitons are known to exist in molecular crystals⁸ and their electronic structure can be described by means of the Wannier picture⁹ with an appropriate static dielectric constant. However, their interaction with the lattice is significantly different from the Wannier excitons found in inorganic semiconducting hosts. The CT exciton binding energy lies in the few-eV range, making them less susceptible to phonon-induced ionization as compared to Wannier excitons in inorganic semiconductors.

In previous work, the linear optical properties of CO-MQWs were measured in some detail.⁷ It was found that the lowest-energy CT exciton absorption line was blueshifted with decreasing well width. This observation is consistent with quantum confinement of the CT exciton by energy wells formed in one of the two MQW layers (consisting of 3,4,9,10-perylenetetracarboxylic dianhydride or PTCDA), sandwiched between layers of a second material (3,4,7,8-naphthalene tetracarboxylic dianhydride or NTCDA) forming energy barriers. A variational study of the dependence of exciton energy on well width indicates that the exciton radius is approximately 15 Å. This number is significantly smaller than that

found in III-V semiconducting compounds because of the smaller static dielectric constant of organic crystals. The strong Coulomb binding energy (as compared with the kinetic energy of each charge carrier) in the CO-MQW materials implies that the quantization due to the well thickness L is determined by the center-of-mass motion of the exciton. Hence the exciton binding energy is given by $\hbar\omega_x = \hbar\omega_B + (\hbar\pi n)^2/2ML^2$ for an infinitely deep potential well, where ω_B is the bulk exciton binding energy, n is an integer, and M is the total mass of the exciton. This expression provides a qualitative explanation of the observed blueshift that was reported in the linear absorption measurements. Since the CT exciton represents a correlated electron-hole pair between nearly adjacent molecules in a stack, we can consider this radius to be the spatial dimension in an electric dipole moment. Such a large dipole moment should, in turn, lead to large optical nonlinearities in these materials. These optical nonlinearities are the focus of this study.

The starting point of our analysis of the optical properties of CT excitons in crystalline organic materials is the Davydov Hamiltonian which describes the interaction of excitons with phonons and external radiation fields. Assuming the rotating-wave approximation, existence of one phonon mode, and keeping only the linear exciton-phonon interaction, the Hamiltonian is

$$H = \hbar(\omega_x - \omega)a^\dagger a + \hbar\omega_0 b^\dagger b - \hbar\lambda a^\dagger a Q - \frac{1}{2}\mu a^\dagger E - \frac{1}{2}\mu a E^*, \quad (1)$$

where $\hbar\omega_x$ and $\hbar\omega_0$ are the quantum-confined exciton binding and phonon energies, respectively. Also, λ is the exciton-phonon coupling constant, μ is the electric dipole moment of the exciton, $a^\dagger a$ and $b^\dagger b$ are the exciton and phonon populations, respectively. Further, $Q = b + b^\dagger$ is the phonon amplitude, E is the slowly varying envelope of the external field, and a and b are the exciton coherence and phonon annihilation operators, respectively.

Careful interpretation of the constants λ and μ must be considered. Current measurements appear to be inconclusive concerning the effects of quantization on these

constants. From a theoretical point of view, quantum confinement should play a role since the envelope wave functions are quantized and they enter in the computation of the matrix elements of the observables. That is, the quantum confinement modifies the bulk values by a factor that reflects the overlap of the spatial wave functions for the electrons and holes.

The temporal evolution of the exciton coherence a and phonon amplitude Q are determined by the Heisenberg equation of motion, and are given by

$$\frac{da}{dt} + [i(\omega_x - \omega) + \gamma]a = i\lambda Qa + i\frac{\mu E}{2\hbar}, \quad (2a)$$

$$\frac{d^2Q}{dt^2} + \Gamma\frac{dQ}{dt} + (\omega_0)^2Q = 2\omega_0\lambda a^\dagger a, \quad (2b)$$

where γ and Γ are phenomenological exciton dephasing and phonon decay rates, respectively. Equations (2) provide insight into the nonlinear optical behavior of exciton-phonon-coupled systems. The term $i\lambda Qa$ in Eq. (2a) is a renormalization of the exciton frequency due to its coupling to the phonon structure of the material. Since it depends on the phonon amplitude Q , the renormalization factor can be seen to be proportional to the exciton density from the steady-state solution of Eq. (2b). This implies that the effective exciton frequency is a function of the population of photogenerated excitons, which is proportional to the light intensity. Hence, optical nonlinearities in these materials have their origin in an exciton-phonon-induced frequency shift,⁵ in a manner similar to the dynamic Stark shift in polaritons.¹⁰

The nonlinear evolution of coupled waves is determined by the Maxwell equations. In the slowly varying envelope approximation, they are given as

$$2ik_a \frac{dE_a}{dz} = - \left(\frac{\omega}{c} \right)^2 P_a, \quad (3a)$$

where the nonlinear polarization density P_a is defined by

$$P_a = N\mu\langle a \rangle. \quad (3b)$$

Here, N is the number density of CT excitons and $\langle a \rangle$ is the expectation value of a . The subscript a denotes the radiation field oscillating at frequency ω_a .

Equations (1)–(3) have exact, closed-form analytical solutions in the steady-state regime. We shall consider three important cases. The first involves the linear response of the medium to an optical radiation field. A comparison of the theoretical model to the available experimental data will provide an estimate of the coupling parameters. Second, we will explore the nonlinear response of the medium by obtaining an exact solution to the CT exciton population $\langle a^\dagger a \rangle$. Finally, we will use the results to understand the process of two-beam coupling¹ in these materials. The latter involves the nonlinear coupling of strong and weak radiation fields.

For the case of a single input optical wave, the analytical solution of Eq. (2) is obtained under the condition of

factorization of the respective variables, a and Q . First, in the low-intensity regime, the population of photogenerated excitons is proportional to the intensity of the optical wave, and the polarization density is determined by the steady-state small-signal solution of Eqs. (2). That is,

$$P = \frac{N\mu^2}{2\hbar} E e^{-i\omega t} \left\langle \left\langle \frac{1}{\omega_x - \omega + i\gamma} \right\rangle \right\rangle. \quad (4)$$

Figure 1 depicts the linear absorption (dark solid line) measurement and the theoretical fit (light solid line) which assumes the existence of two excitonic lines in the S_0 to S_1 electronic manifold.⁸ The theoretical result is fitted against the experimental data in the following manner. The wavelengths of the two maxima located in the right-hand side of the experimental absorption profile are chosen to set the horizontal scale. The vertical scale is set by the ratio of the two peaks in the right-hand side of the data, assuming that the height of the largest peak is equal to unity. In order to obtain reasonably good quantitative agreement, the imaginary part of the polarization density was averaged over a Maxwellian distribution with two distinct widths, which are chosen from the experimental data. The use of the Maxwellian distribution is consistent with the fast phonon-induced relaxation processes that exist in these materials. The result shown in Fig. 1 indicates that the experimental data contain more than two excitonic lines, which is the source of discrepancy between the theoretical model and experimental data. In spite of the complexity, the theoretical model gives an adequate understanding of the origin of the linear absorption spectra of these materials.

Second, in the fully nonlinear regime, the solution for the population $\langle a^\dagger a \rangle$ of the CT exciton is given by the

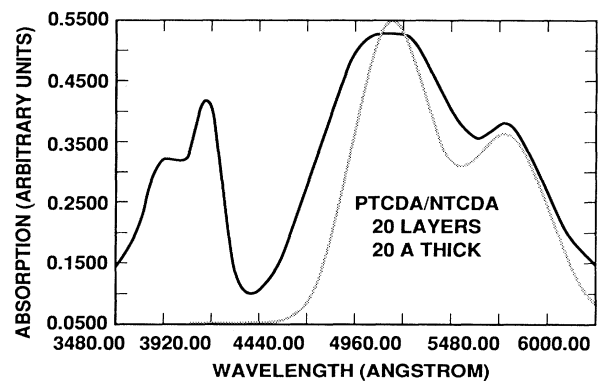


FIG. 1. Linear absorption coefficient of PTCDA/NTCDA MQWs. The experimental data (dark solid line) contain two additional sidebands on the left-hand side due to the presence of the NTCDA. The theoretical fit (light solid line) from the solution of the exciton-phonon equations is based on thermalization by phonons and the assumption of two exciton resonances.

cubic equation

$$\langle a^\dagger a \rangle = \frac{\Omega^2}{\gamma^2 + [\Delta - (2\lambda^2/\omega_0)^2 \langle a^\dagger a \rangle]^2}, \quad (5)$$

where $\Delta = \omega_x - \omega$ is the detuning from the exciton resonance and $\Omega = \mu E/2\hbar$ is the Rabi frequency. Figure 2 shows the solution of this cubic equation as a function of the Rabi frequency for different values of the detuning parameter Δ . In this plot, all physical variables have been normalized to $2\lambda^2/\omega_0$. A transition to multivalued behavior is observed for a sufficiently large value of the detuning parameter Δ . This behavior can be understood in the following manner. Multivalued behavior of Eq. (5) is achieved if the derivative of the Rabi frequency with respect to the exciton population changes sign. A simple calculation of this criterion asserts that bistability is present provided that

$$\Delta > \sqrt{3}\gamma. \quad (6)$$

This condition is valid even in the absence of an optical cavity. Hence, the coupled exciton-phonon system possesses the property of intrinsic bistable behavior which arises from the renormalization of the exciton frequency mediated by the exciton-phonon interaction.

Finally, we consider the interaction between a strong wave E_0 , oscillating at frequency ω , and a weak wave E_1 , oscillating at frequency $\omega + \delta$. Their nonlinear coupling yields a coherent traveling-wave excitation in the medium oscillating at frequency δ . The scattering of the strong wave from the coherent excitation changes the absorption coefficient and the index of refraction experienced by the weak wave. A calculation of the optical

response function in the undepleted pump approximation gives the following expression for the spatial evolution of the weak wave:

$$\frac{1}{E_1} \frac{dE_1}{dz} = -\frac{\omega + \delta}{2n_1} \frac{N\mu^2\omega_0}{\epsilon_0\hbar 2\lambda^2} (a + i\beta), \quad (7a)$$

where the dimensionless (all physical parameters are normalized to $2\lambda^2/\omega_0$) nonlinear absorption coefficient α is

$$\alpha = \frac{(\omega_0^2 - \delta^2)C - \delta\Gamma D}{C^2 + D^2} \quad (7b)$$

and the dimensionless nonlinear index of refraction is given by

$$\beta = \frac{(\omega_0^2 - \delta^2)D + \delta\Gamma C}{C^2 + D^2}, \quad (7c)$$

with the following expressions for C and D :

$$C = \gamma(\omega_0^2 - \delta^2) + \delta\Gamma(\Delta - \delta) - \delta\Gamma\langle a^\dagger a \rangle,$$

$$D = (\omega_0^2 - \delta^2)(\Delta - \delta) - \delta\Gamma\gamma - (2\omega_0^2 - \delta^2)\langle a^\dagger a \rangle.$$

Figure 3 shows the behavior of the nonlinear absorption coefficient, $\alpha + i\beta$, of the weak wave as a function of the Rabi frequency induced by the strong wave for different values of the quantum-well dimension. A transition to bistable behavior, accompanied by gain (negative values of the nonlinear absorption coefficient) of the weak wave at the expense of the strong wave, is observed for a critical value of the normalized Rabi frequency and a small enough value of the quantum-well dimension. The dimension of the quantum well plays a key role in

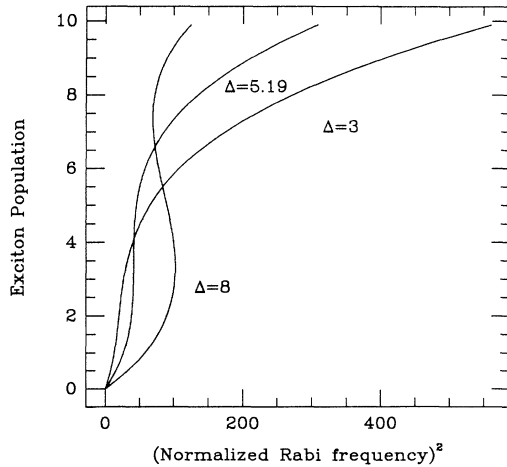


FIG. 2. Dependence of the exciton population on the normalized Rabi frequency to the second power. The linewidth and the detuning are also normalized to $2\lambda^2/\omega_0$, which has the unit of frequency. Curves are shown for normalized detuning $\Delta=3$, $\Delta=5.19$, which corresponds to the transition region for bistability to begin taking place, and $\Delta=8$.

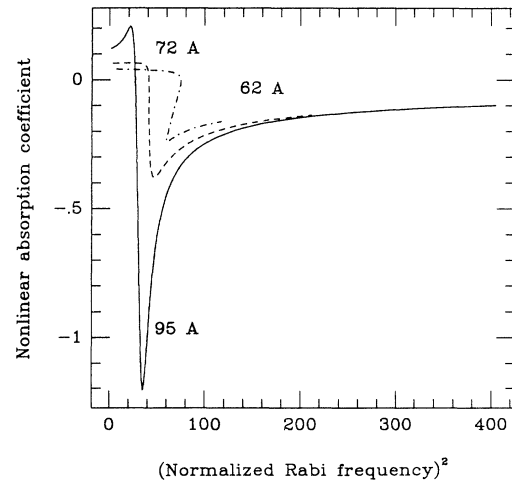


FIG. 3. Two-wave-mixing gain (negative value) and absorption (positive value) coefficient for three different values of the quantum-well size. Prediction of optical bistability and energy transfer is given for $L=62$ Å. The normalized probe-pump detuning parameter δ is set equal to -1 .

the detuning parameter Δ . For large enough detuning or small enough well size, the value of the detuning parameter satisfies the bistability condition (6). Hence, a coherent energy transfer from the strong to the weak wave takes place with a threshold behavior. This phenomenon can be thought of as a coherent bistable optical switch. That is, the energy transfer takes place from the strong to the weak optical beams when a certain threshold is achieved. The bistable behavior is a reflection of the nonlinear functional dependence of the exciton population on the pump intensity.

The phenomena discussed in the previous paragraphs provide insight into subtle effects that appear in the Davidov Hamiltonian. Estimates of the physical parameters such as λ and ω_0 are crucial to the understanding of the materials growth conditions as well as to the future applications of these novel materials for optoelectronics. The beauty and simplicity of our results are contained in one single physical parameter, the Franck-Condon (FC) shift. This frequency shift is related to λ and ω_0 by the following expression:

$$\text{FC} = \lambda^2 / \omega_0,$$

and is a measure of the degree of reduction of the potential energy of the material due to the exciton-phonon coupling. From measured values in aromatic molecules,¹¹ λ is approximately equal to ω_0 . These numbers imply a FC shift of 700 cm^{-1} for the case of naphthalene compounds.

It is interesting to calculate the range of laser powers required to observe the onset of optical bistability and two-beam energy transfer. However, the nonlinear absorption coefficient is a sensitive function of the material parameters. For example, if one assumes a FC shift of approximately 1000 cm^{-1} expected for large molecules such as PTCDA,¹² an oscillator strength of unity (consistent with the observed large linear absorption coefficients of 10^5 cm^{-1}), a normalized exciton dephasing rate ranging from 10^{-3} to 1, one finds that the power density ranges from 100 to 10^6 W/cm^2 for $\Delta = 10^{-3} \text{FC}$.

A more accurate value must wait for a detailed measurement of the FC shift, and the exciton dephasing rate.

In summary, we presented new results on the optical behavior of these newly discovered materials. We predict the existence of intrinsic bistability as well as a coherent energy transfer from a strong wave to a weak wave. The energy exchange occurs under bistable conditions, leading to the possibility of novel optical devices using these materials.

This work is supported by the Air Force Office of Scientific Research (Dr. Howard Schlossberg and Major G. Pomrenke). One of us (J.F.L.) would like to thank Dr. R. N. Schwartz for enlightening discussion on organic materials.

¹See *Nonlinear Optics of Organics and Semiconductors*, edited by T. Kobayashi (Springer-Verlag, Berlin, 1989).

²M. Sinclair, D. Moses, A. J. Heeger, K. Vilhelmsson, B. Valk, and M. Salour, *Solid State Commun.* **61**, 221 (1987).

³See *Nonlinear Optical Properties of Organic Molecules and Crystals*, edited by D. S. Chemla and J. Zyss (Academic, New York, 1987).

⁴W. P. Su, J. R. Schrieffer, and A. J. Heeger, *Phys. Rev. Lett.* **42**, 1698 (1979); L. Rothberg, T. M. Jedju, S. Etemad, and G. L. Baker, *Phys. Rev. Lett.* **57**, 3229 (1986).

⁵B. I. Greene, J. F. Mueller, J. Orenstein, D. H. Rapkine, S. Schmitt-Rink, and M. Thakur, *Phys. Rev. Lett.* **61**, 325 (1988).

⁶S. A. Brazovskii and N. N. Kirova, *Pis'ma Zh. Eksp. Teor. Fiz.* **33**, 6 (1981) [*JETP Lett.* **33**, 4 (1981)].

⁷F. F. So, S. R. Forrest, Y. Q. Shi, and W. H. Steier, *Appl. Phys. Lett.* **56**, 674 (1990).

⁸M. Pope and C. E. Swenberg, *Electronic Processes in Organic Crystals* (Oxford Univ. Press, New York, 1982).

⁹P. J. Bounds and W. Siebrand, *Chem. Phys. Lett.* **75**, 414 (1980).

¹⁰A. L. Ivanov and L. V. Keldysh, *Zh. Eksp. Teor. Fiz.* **84**, 404 (1983) [*Sov. Phys. JETP* **57**, 234 (1983)].

¹¹V. L. Broude, E. I. Rashba, and E. F. Sheka, *Spectroscopy of Molecular Excitons* (Springer-Verlag, Berlin, 1985).

¹²D. Haarer and N. Karl, *Chem. Phys. Lett.* **21**, 49 (1973).